

Published in final edited form as:

J Immunol. 2009 June 1; 182(11): 7190–7200. doi:10.4049/jimmunol.0802562.

Myeloid-Specific Deletion of Tumor Suppressor PTEN Augments Neutrophil Transendothelial Migration during Inflammation¹

Bara Sarraj^{*}, Steffen Massberg[†], Yitang Li^{*}, Anongnard Kasorn^{*}, Kulandayan Subramanian^{*}, Fabien Loison^{*}, Leslie E. Silberstein^{*,†}, Ulrich von Andrian[†], and Hongbo R. Luo^{*,†,2}

^{*}Department of Lab Medicine, Children's Hospital, Boston, MA 02115

[†]Department of Pathology, Harvard Medical School, Boston, MA 02115

Abstract

Phosphatidylinositol 3,4,5-trisphosphate (PIP₃) is a second messenger that is involved in a number of cell activities including cell growth, proliferation, and motility. PIP₃ is produced by PI3K and regulated by PTEN (phosphatase and tensin homolog deleted on chromosome 10) and SHIP lipid phosphatases. Evidence from our experiments shows that enhanced PIP₃ production results in elevated neutrophil recruitment under inflammatory conditions. However, the mechanism of this elevation is not well understood. We used intravital video microscopy to investigate neutrophil recruitment in the cremaster venules of wild-type and PTEN knockout (KO) mice. Neutrophil transmigration was augmented in PTEN KO mice 4 h after TNF- α intrascrotal injection. PTEN KO neutrophils also showed significantly enhanced transmigration 2 h after MIP-2 intrascrotal injection, an effect that dramatically decreased when PI3K or Src kinase inhibitor treatments preceded MIP-2 stimulation. Similarly, fMLP superfusion of the cremaster muscle lead to enhanced emigration in PTEN KO mice. The observed elevation in neutrophil emigration was likely caused by increased speed of crawling, crossing the venular wall, and migrating through the muscular tissue in PTEN KO mice because the effect of PTEN depletion on neutrophil rolling or adhesion was minimal. Interestingly, chemoattractant-induced release of gelatinase and elastase was also elevated in PTEN null neutrophils, providing a potential mechanism for the enhanced neutrophil migration in the PTEN KO mice. Collectively, these results demonstrate that PTEN deletion in neutrophils enhances their invasivity and recruitment to inflamed sites more likely by raising the cell physical capability to cross the vascular and tissue barriers.

The recruitment and activation of neutrophils are important mechanisms of the innate immune system. Neutrophils migrate from the blood to infected tissues by responding to a variety of chemokines, leukotrienes, complement peptides, and some chemicals released by bacteria directly, such as peptides bearing the N-formyl group (formyl peptides) (1–3). These responses are mediated by a network of intracellular signaling pathways. One essential component in this network is phosphatidylinositol 3,4,5-trisphosphate (PIP₃),³ an inositol phospholipid that can be produced in response to various stimuli, including

¹This work is supported by Grant HL066987 from the National Institutes of Health Training Program (to B.S.). This work is also supported by Grants AI076471, HL085100, and GM076084 from the National Institutes of Health (to H.L.) and a Research Scholar Grant from the American Cancer Society.

Copyright © 2009 by The American Association of Immunologists, Inc.

²Address correspondence and reprint requests to Dr. Hongbo R. Luo, Department of Laboratory Medicine, Karp Family Research Building, Room 10214, Children's Hospital, Boston, MA 02115. Hongbo.Luo@childrens.harvard.edu.

Disclosures

The authors have no financial conflict of interest.

guanosine nucleotide-coupled receptor activation, integrin ligation, receptor tyrosine kinase activation, and shear stress (4–7). PIP₃ exerts its function by mediating protein translocation via pleckstrin homology domains on the protein (8, 9). A subset of pleckstrin homology domains, including those in Btk, protein kinase B/Akt, phospholipase C- γ , Gab1, phosphoinositide-dependent kinase 1, and Grp-1, drive membrane translocation of their host proteins through specific, high-affinity recognition of PIP₃ (10). This membrane translocation is crucial for these proteins to fulfill their functions in various cellular processes such as cell survival, proliferation, growth, differentiation, and membrane trafficking. PIP₃ also augments the activity of guanosine exchange factors, and subsequently activates CDC42, Rac, and Rho GTPases that control the formation of filopodia, lamellipodia, and actin stress fibers and regulate cell adhesion, polarization, chemotaxis, and cytoskeletal rearrangement in neutrophils (10–14).

PIP₃ is synthesized by the enzyme PI3K. Using different approaches, a number of studies demonstrated that blocking the kinase activity of PI3K led to impaired neutrophil migration in vitro and decreased neutrophil recruitment to inflammatory sites in vivo (15–22). PIP₃ level can also be regulated by PTEN (phosphatase and tensin homolog deleted on chromosome 10), which was first identified as a tumor suppressor gene (23, 24) and then subsequently shown to be a phosphatidylinositol 3'-phosphatase that dephosphorylates PIP₃ to phosphatidylinositol 4,5-bisphosphate (PIP₂) (25). Elevation of PIP₃ signaling via depleting PTEN enhances cell mobility in various cell types, including fibroblasts (14), T cells (26), eosinophils (27), and several cell lines (28, 29). Recently, we demonstrated that depletion of PTEN enhances the membrane translocation of PIP₃-specific pleckstrin homology domain in neutrophils, thus augmenting the PIP₃ down-stream signals, leading to enhanced sensitivity to chemoattractant stimulation, elevated superoxide production, and enhanced neutrophil chemotaxis. In addition, neutrophil recruitment to inflamed peritoneal cavity was significantly elevated in the PTEN knockout (KO) mice (30).

Neutrophil migration through blood vessel wall is a complex process that can be divided into at least four discrete phases: capture and rolling, activation, arrest or firm adhesion, and diapedesis or transmigration from circulation across endothelium into tissues (31–40). Which step is enhanced and responsible for the observed elevation of neutrophil recruitment in the PTEN KO mice is still largely unknown. In this study, we have investigated the multistep recruitment of neutrophil in a mouse cremaster muscle using intravital video microscopy (IVM). We found that PTEN disruption significantly enhanced neutrophil recruitment in the cremaster muscle in response to different stimuli. Enhanced recruitment was associated with faster neutrophil movement in the vascular bed, across the vascular endothelial wall, and in the muscle tissue. Hence, we propose that PTEN is a negative regulator in neutrophil trafficking and should be a legitimate therapeutic target for modulating neutrophil recruitment in a variety of infectious and inflammatory diseases.

Materials and Methods

Mice and reagents

Myeloid-specific deletion of PTEN was performed as previously described (41). Age-matched, 10- to 14-wk-old, male wild-type (WT) mice and PTEN KO (PTEN^{loxP/loxP} Cre^{+/+} or PTEN^{loxP/loxP} Cre^{+/-}) mice were used in all experiments. The study protocol was approved by the Animal Care and Use Committee of Children's Hospital Boston. MIP-2 and TNF- α were purchased from R&D Systems. fMLP, rhodamine 6G, LY942002, a PI3K

³Abbreviations used in this paper: PIP₃, phosphatidylinositol 3,4,5-trisphosphate; PIP₂, phosphatidylinositol 4,5-bisphosphate; PSGL, P-selectin glycoprotein ligand; IVM, intravital video microscopy; KO, knockout; WT, wild type; PTEN, phosphatase and tensin homolog deleted on chromosome 10.

inhibitor, and PP2, a Src tyrosine kinase inhibitor were purchased from Sigma-Aldrich. FITC- or PE-conjugated anti-mouse Gr-1 mAbs (clone RB6-8C5), PE-conjugated anti-mouse CD62L, P-selectin glycoprotein ligand (PSGL)-1, CD11b, and CD18 mAbs, FITC-conjugated anti-mouse CD44 and CD29 mAbs, and Alexa Fluor 488-conjugated anti-mouse CD31 mAb (clone 390) were purchased from BD Biosciences or BioLegend.

Cremaster muscle preparation

The surgical procedure to expose the cremaster muscle was performed as previously described (17, 42–44) with slight modification. Mice were i.p. anesthetized with a mix of 200 μg of ketamine/20 μg of xylazine per mouse every 45 min until the end of the experimental period. The hair covering the right testes area was shaved with an electric razor and hair removal lotion. A diagonal incision was made starting at the tip of the testis that was exposed on a Plexiglas custom-built stage. A longitudinal incision was made at the ventral side of the muscle using a heat cauterizer, and the muscle was spread using 6–0 sutures. The muscle was continuously superfused with 35°C thermostable 0.09% saline solution. Temperature at the muscle surface was frequently checked by a digital thermometer probe. The surgical procedure takes ~13 min.

IVM acquisition

The preparation was transferred to an intravital microscope (IV-500; Micron Instruments) with epifluorescence capability. Digital recording of videos was acquired by QED Imaging software (MediaCybernetics). At least three vessels of 20- to 40- μm diameter were recorded per time point. A waiting period of 15 min was observed to stabilize blood flow before any recording was taken. For fMLP (final concentration, 10 μM) superfusion preparation, control recordings were taken ahead of applying the chemoattractant superfusion. For TNF- α preparation, the mouse was intrascrotally injected with 0.5 μg of TNF- α in 300 μl of sterile saline solution at 2 and 4 h before start of recording. For MIP-2 preparation, the mouse was intrascrotally injected with 1 μg of MIP-2 in 300 μl of sterile saline solution at 2 h ahead of video acquisition. PI3K inhibitor LY942002 (10 mg/kg) or Src inhibitor PP2 (0.2 mg/kg) (45) was i.v. introduced 15 min ahead of MIP-2 intrascrotal injection. To induce ischemia (46, 47), a metal clamp (Fine Science Tools) was inserted at the muscle base under saline superfusion; blood flow blockage was confirmed using IVM. The clamp was removed 30 min later and the blood flow was allowed for additional 60 min under the same superfusion conditions. To observe the blood flow center-line velocity, 100 μl of rhodamine 6G (2 mg/ml) was i.v. injected. To confirm that leukocytes observed under brightfield are neutrophils, 4 μg of FITC-conjugated anti-Gr-1 mAb in 100 μl of saline solution were i.v. injected, and leukocyte trafficking was visualized immediately. To delineate the endothelial cell boundaries, 40 μg of Alexa Fluor 488-conjugated anti-CD31 (PECAM-1) mAb in 150 μl of saline solution was i.v. injected. Videos of 30–60 s were recorded under 40X water-immersion objective with a frame rate of 10 frames/s and 1 or 2 binning. For crawling and vascular wall crossing, videos of 5–10 min were recorded under $\times 40$, $\times 63$, and $\times 100$ magnification with a frame rate of 5 frames/s and 2 binning. Epifluorescent videos were taken at 56 frames/s and 2 binning (CD31) and 96 frames/s and 4 binning (rhodamine 6G).

IVM analysis

Offline analysis of recorded videos was performed by frame-by-frame playback using Quicktime software. Rolling cells were defined as the cells moving over the 100- μm long vessel with a velocity below the velocity of RBC. Adherent cells were defined as cells staying still for at least 30 s. Emigrating cells were calculated as the number of cells that left completely the blood vessel and still within a distance of 50 μm on both sides, thus in an area $100 \times 50 \times 2 \mu\text{m}$ or $10^4 \mu\text{m}^2$. Crawling cells were considered the cells moving slowly on the vessel bed with a polarized phenotype. To calculate the speed at which a cell crosses

the vascular wall, we measured the distance between the cell head when it first shows up at the vessel abluminal side and the cell head when the tail just detached from the abluminal side of the vessel. Rolling velocity (10 cells/vessel) was measured as the distance (in micrometers) between two points over time (seconds). Crawling as well as tissue emigration velocity were measured for cell straight movements (in micrometers) only, between two points over time (seconds). Centerline blood velocity (V_{rbc}) was measured for 20 cells/vessel under a high recording rate of 96 frames/s. Mean blood flow velocity was calculated as centerline velocity at 0.625 (48). Wall shear rate was calculated as 8×2.12 (mean blood velocity per diameter) (48, 49).

Blood count and histology

Blood was collected at the end of every preparation from the eye retro-orbital sinus into EDTA-coated tubes (BD Biosciences) and differential count was measured by Hemavet 850 (Drew Scientific). At the end of experiment, cremaster muscle was fixed overnight in 4% paraformaldehyde at 4°C, paraffin-embedded, sectioned and stained with H&E.

Electron microscopy

MIP-2 (1 $\mu\text{g}/300 \mu\text{l}$ of saline) was injected intrascrotally and the cremaster muscle was dissected 3 h later. Tissue was fixed overnight in 2.5% formaldehyde, 5.0% glutaraldehyde, 0.06% picric acid in 0.2 M cacodylate buffer; all reagents were purchased from Electron Microscopy Sciences. Tissue was then washed several times in 0.1 M cacodylate buffer and osmicated in a final solution of 1% osmium tetroxide and 1.5% potassium ferrocyanide for 3 h, followed by several washes of dH_2O . One percent of uranyl acetate in maleate buffer is added for 1 h, and tissue was washed several times with maleate buffer (pH 5.2). This process is followed by a graded cold ethanol washing series (50%, 80%, 95%, and 100% ethanol) over 1 h. Propylene oxide washes follow, again three times over 1 h. Then tissue was placed in 1:1 mixture of propylene oxide and plastic, including catalyst, overnight, embedded in pure plastic Taab resin (Marivac) the next day and put into 60°C oven for 1 or 2 days. The 95-nm sections were cut with Leica ultracut microtome, picked up on Formvar-coated copper grids, stained with 0.2% lead citrate, and viewed and imaged under the Philips Technai Spirit Electron Microscope.

Flow cytometry

Blood was collected from the eye retro-orbital sinus, and RBC were lysed at room temperature in an ACK lysing buffer (Invitrogen). After being washed in a washing buffer (Dulbecco's PBS, 1% BSA and 0.09% NaN_3), cells were then incubated with Fc block (anti-CD16/CD32) for 15 min followed by fluorescent-conjugated Abs (1 $\mu\text{g}/1$ million cells) for 30 min at 4°C. Cells were then washed and fixed in 4% paraformaldehyde. Flow cytometry was performed using a FACSCanto II machine (BD Biosciences) and analyzed using Flowjo software (Tree Star). For fMLP stimulation in vitro, 5×10^5 WT or PTEN KO bone marrow leukocytes (in RPMI 1640 medium, 0.25% BSA) were stimulated with 500 nM fMLP for 0, 1, and 5 min. Equal volume of 7.4% formaldehyde was added, and cells were kept on ice for 20 min. Cells were then double stained with FITC-Gr-1 and PE-CD11b as above.

Chemoattractant-induced elastase and gelatinase release from neutrophils

Mouse bone marrow-derived neutrophils were resuspended at a density of $1 \times 10^7/\text{ml}$ in HBSS (with calcium/magnesium, no FCS), and then stimulated with fMLP (1 μM) for 30 min at 37°C. Supernatants were harvested and gelatinase and elastase activities in the supernatants were measured using EnzChek Gelatinase Assay kit (Molecular Probes) and EnzCheck Elastase Assay kit (Molecular Probes), respectively, according to protocols provided by the manufacturer's. In both assays, the samples were incubated for 5 h at room

temperature. Fluorescence was measured in a fluorescence multiwell plate reader set for excitation at 485 ± 10 nm and emission detection at 530 ± 15 nm. Background fluorescence has been subtracted from each value. Cell lysates of the same number of unstimulated neutrophils were used to measure the total amount of intracellular gelatinase and elastase activity.

Statistical analysis

We used the Student *t* test (Microsoft Excel) for data analysis. A value for $p < 0.05$ defined statistical significance.

Results

Examination of leukocyte transendothelial migration using IVM

PTEN null neutrophils displayed enhanced accumulation in the mouse peritoneum in response to inflammatory stimulants such as *Escherichia coli* or thioglycolate (30). To understand the mechanism of this accumulation, we dissected the steps that neutrophils take to leave the circulation into their accumulation endpoint. We used brightfield and epifluorescent IVM to observe the leukocyte behavior in the postcapillary venules in the mouse cremaster muscle. Leukocyte recruitment was induced by intrascrotal injection of MIP-2, a neutrophil chemoattractant, or TNF- α , an inflammatory cytokine. It was reported previously that most transmigrated leukocytes in this system are neutrophils (16, 50–52). This finding was confirmed in our system using three independent approaches. Traditional histological analysis of the mouse cremaster muscle showed that the majority of cells (96%) recruited were multilobed nucleated neutrophils in both WT and PTEN KO mice (see supplemental Fig. S1, A and B).⁴ Consistently, epifluorescent IVM showed that most transmigrating cells (90%) were Gr-1-positive cells that were stained by i.v. injected FITC-conjugated anti-Gr-1 mAb (data not shown). Finally, electron microscopy also showed that more than 98% of cells recruited were neutrophils in both WT and PTEN KO mice (see supplemental Fig. S1, A and B).⁴ Therefore, the trafficking parameters measured in this system should authentically reflect the behavior of neutrophils.

PTEN null neutrophils display enhanced emigration in response to fMLP superfusion

Conventional *Pten*^{-/-} mice die in early embryonic stage. Thus, we used a conditional myeloid-specific PTEN KO mouse in which PTEN deletion only occurs in the myeloid lineage, including monocytes, mature macrophages, and neutrophils (30). The depletion of PTEN protein in neutrophils was confirmed by Western blot analysis. In addition, specific increase in PIP₃ signaling was confirmed by measuring phosphorylation of Akt, a well-known downstream factor in the PIP₃ signaling pathway (see supplemental Fig. S2).⁴ We first studied the neutrophil trafficking behavior in response to fMLP, a chemoattractant peptide released by bacteria and considered as a bacterial endpoint stimulant. WT and PTEN KO mice had similar blood neutrophil counts, and their cremaster postcapillaries displayed similar wall shear rates (see supplemental Table S1).⁴ In naive (unchallenged) mice, WT and KO neutrophils had minimal adhesion and emigration capability due to lack of stimulation (see supplemental Table S5).⁴ The neutrophil rolling was likely a result of tissue trauma caused by surgery. In fMLP-superfused venules, the number of adherent neutrophils was significantly increased, but was comparable between the WT and PTEN KO mice over the 1-h observation period (Fig. 1C). PTEN KO neutrophils were slightly faster in rolling at the 20- and 60-min time points (Fig. 1B), whereas the number of rolling cells is similar to each other (Fig. 1A). In addition, PTEN KO neutrophils showed much more pronounced

⁴The online version of this article contains supplemental material.

emigration capability over the 1-h stimulation (Fig. 1D). At 20 min of fMLP superfusion, ~10 emigrated neutrophils and at 40 min, ~20 emigrated neutrophils were detected in a $10^4 \mu\text{m}^2$ area close to the vessels in the PTEN KO mice. By contrast, only about two neutrophils at 20 min and three neutrophils at 40 min were detected in the WT mice. Because there was no significant difference in venule dimension and blood neutrophil count between the WT and PTEN KO mice (see supplemental Table S2A),⁴ the elevated neutrophil emigration was likely directly caused by the cellular alterations in neutrophils.

PTEN KO neutrophils display enhanced emigration in response to intrascrotally injected TNF- α or MIP-2

The early (~1 h) and prolonged (4–5 h) responses to inflammatory stimuli might be mediated by distinct cellular pathways. For instance, Liu et al. (17) recently reported that the early response of neutrophils to MIP-2 or KC is mediated by PI3K γ , whereas the more prolonged response to MIP-2 or TNF- α is mediated by PI3K δ . To investigate whether PTEN depletion can also alter neutrophil trafficking over a relatively longer period of time, we intrascrotally injected TNF- α (0.5 μg) and then observed the leukocyte behavior at 2- and 4-h time points. PTEN KO neutrophils displayed higher rolling influx at 0- and 4-h time points with a small but statistically significant decline at the 2-h time point (Fig. 2A). Similar with what was observed in fMLP-stimulated mice, PTEN KO neutrophils were faster in rolling until they converged after 4 h into a similar rolling speed with WT neutrophils (Fig. 2B). The number of neutrophils adhering to the vascular endothelium was slightly increased after 4 h of TNF- α introduction (Fig. 2C), whereas the emigration of PTEN KO neutrophils was dramatically enhanced (Fig. 2D). Again, there was no significant difference in venule dimensions and in blood neutrophil count after these experiments (see supplemental Table S2B).⁴

To examine whether the enhancement of neutrophil emigration is a general phenotype caused by PTEN-depletion, we further investigated neutrophil recruitment induced by intrascrotal injection of MIP-2 (CXCL2), a neutrophil chemoattractant that is up-regulated in the vascular lumen in response to inflammatory stimuli such as TNF- α (52). MIP-2 is often considered as an intermediate inflammatory stimulant. In response to MIP-2, there was no difference in rolling influx, rolling velocity, or adhesion between WT and PTEN KO neutrophils (Fig. 3, A–C). In contrast, at 2 h after MIP-2 injection emigration of neutrophils was significantly enhanced in the PTEN KO mice (Fig. 3D). Collectively, our results demonstrated that PTEN acts as a negative regulator in neutrophil transendothelial migration.

Enhanced neutrophil emigration in PTEN KO mice could be inhibited by PI3K inhibitor in vivo

PTEN is a lipid phosphatase that negatively regulates PIP₃ signaling (25). Consistently, PIP₃ signal was dramatically elevated in the PTEN null neutrophils (30). To examine whether the observed enhancement of neutrophil emigration in PTEN KO mice is a direct result of augmented PIP₃ signal, we investigated whether this enhancement can be inhibited by LY942002, a PI3K inhibitor (Fig. 3A). In comparison to MIP-2 treatment only, PI3K inhibition by LY942002 did not significantly affect neutrophil rolling speed or adhesion in either WT or PTEN KO mice, and rolling influx was only slightly reduced (Fig. 3, B–D). However, neutrophil emigration was dramatically lowered by LY942002 treatment in both WT and PTEN KO mice (Fig. 3E). This inhibition is likely due to the direct suppression of intracellular signaling pathways involved in neutrophil trafficking because PI3K inhibition had no effect on the expression level of L-selectin, PSGL-1, and CD11b on either WT or PTEN KO neutrophils (data not shown). Interestingly, PP2 also significantly blocked neutrophil emigration in WT and PTEN KO mice (Fig. 3A). Thus, the PTEN depletion–

induced enhancement of neutrophil recruitment was completely abolished after PP2 treatment. No significant difference in neutrophil emigration was detected between PP2-treated WT and PP2-treated PTEN KO mice (Fig. 3E). These results suggest that Src family tyrosine kinase might be one of the essential downstream targets mediating PIP₃ signaling during neutrophil transmigration. There was no significant difference in venule dimensions or blood neutrophil count after these experiments (see supplemental Table S2C).⁴

PTEN KO neutrophils displayed faster crawling and emigration across the postcapillary venular wall and through muscle tissue

Because the number of adherent neutrophils was not significantly increased in the PTEN KO mice, the enhanced neutrophil emigration in these mice was likely due to increased efficiency of steps after adhesion. Thus, we explored whether these steps were affected by PTEN disruption. Recently, it has been suggested that adherent neutrophils crawl on the endothelial cells before their transmigration, presumably to find a “soft spot” (40, 51, 53, 54). Crawling cells are distinguished by their polarized shape and often lateral movement. We measured the speed of crawling by following their movements over the vascular bed in response to fMLP superfusion or MIP-2 intrascrotal injection. The video captions (Fig. 4A) tracks a PTEN KO neutrophil before (Fig. 4, *left*), after wall crossing (Fig. 4, *middle*) and far after detaching into tissue (Fig. 4, *right*). This cell needed ~53 s to negotiate its ~15- μ m body length across the vascular wall. Compared with WT neutrophils, the crawling speed of PTEN KO neutrophils significantly increased from 280 ± 24 nm/s to 400 ± 22 nm/s in response to fMLP, and from 262 ± 45 nm/s to 480 ± 54 nm/s in response to MIP-2 (Fig. 4, B and C). We also calculated the speed at which leukocytes transmigrated cross the vascular endothelial wall and the speed of migration in the tissues after the detachment from the vascular endothelial wall (Fig. 4A and see supplemental Video S1).⁴ They were all dramatically elevated in the PTEN KO mice (Fig. 4, B and C and see supplemental Table S3).⁴ When the transmigration was induced by fMLP superfusion, it took the WT neutrophil 108 ± 22 s to cross the endothelial wall, whereas it only took the PTEN KO neutrophil 60 ± 8 s to cross. Similarly, WT neutrophils emigrated at 247 ± 27 nm/s, whereas PTEN KO neutrophils emigrated at 412 ± 26 nm/s through the extravascular tissue. Similar results were obtained when the transmigration was induced by MIP-2 intrascrotal injection (see supplemental Videos S2 and S3).⁴ Because crawling, crossing vascular endothelial wall, and migration in the tissues are steps that are taken in chronological order, the slight velocity depression in crossing the wall compared with crawling or tissue crossing (more visible in response to MIP-2) describes extra time cells need to cross the vascular barrier, strikingly in a smooth and undisrupted manner (add this to result section). Collectively, these results suggested that disruption of PTEN generally increased the speed of neutrophil migration before, during, and after the tranendothelial migration.

Electron microscopy imaging of the MIP-2-stimulated cremaster vessels revealed that some transmigrating neutrophils were captured on the abluminal side of the vessel between the endothelium and the basement membrane/pericyte layers (Fig. 5, A and B). These cells were most likely in transit out into the tissue. In PTEN KO mice, the number of these transit cells was dropped significantly from 14.5 ± 2.8 cells/mm to 5.8 ± 2.5 cells/mm, which is consistent with the increased neutrophil transmigration speed observed in these mice (Fig. 5, B and C).

PTEN disruption did not alter the preference toward paracellular pathway in neutrophil transendothelial migration

We have shown so far that PTEN KO neutrophils displayed enhanced emigration in response to various stimuli (fMLP, TNF- α , and MIP-2). Leukocytes follow two paths to cross the vessel wall, paracellular pathway through the interendothelial junctions and

transcellular pathway across the endothelial cell itself (55, 56). It was reported that neutrophils predominantly use the paracellular pathway during their transendothelial migration (55). To examine whether PTEN disruption can change such preference, we quantified the percentage of neutrophils undertaking paracellular and transcellular pathways in WT and PTEN KO mice. We superfused the cremaster venules with fMLP and i.v. injected fluorescein-conjugated anti-CD31 (PECAM-1), which is a member of Ig superfamily expressed predominantly at endothelial tight junctions (47, 57). We first delineated the vascular endothelial boundaries by fluorescent imaging and then traced the localization of firmly arrested leukocytes. Endothelial cells displayed the cobblestone diamond-shaped architecture (Fig. 6A and see supplemental Video S4)⁴ and there was no difference in the endothelial cell dimensions between WT and KO vascular beds (see supplemental Table S4).⁴ Firmly adherent cells localized predominantly (>90%) to the endothelial boundaries or tricellular junctions in both WT and PTEN KO mice (Fig. 6B), demonstrating that PTEN disruption did not change the preference toward neutrophil interaction with the paracellular junctions. However, we cannot exclude the possibility that PTEN disruption might also enhance neutrophil transmigration via elevating transcellular pathway.

PTEN KO neutrophils displayed increased transmigration efficiency in ischemia/reperfusion injury

When neutrophil migration was induced by fMLP superfusion or intrascrotal injection of MIP-2 or TNF- α , PTEN depletion significantly enhanced the emigration efficiency. We next examined neutrophil trafficking in a more physiologically relevant setting in which neutrophil migration was induced by an ischemia/reperfusion injury, a condition associated with a number of human diseases such as stroke, heart infarction, or organ transplant (37, 58). To induce ischemia/reperfusion injury, the cremaster underwent 30 min of ischemia followed by 60 min of reperfusion. There was no significant difference in rolling influx between WT and PTEN KO mice (Fig. 7A). Consistent with previous results, neutrophil emigration efficiency was increased by nearly 2-fold from 79.6 ± 20.1 to 167 ± 32.7 in the PTEN KO mice compared with the WT mice at 60 min after reperfusion. Interestingly, unlike what was observed in previous experiments, the number of adherent cells was significantly reduced in the ischemia/reperfusion-challenged PTEN KO mice in comparison with the WT mice receiving the same challenge (Fig. 7B). This reduction might be a result of elevated emigration that drained the vascular bed (Fig. 7, B–D). There was no significant difference in venule dimensions or blood neutrophil count after these experiments (see supplemental Table S2, D).⁴

PTEN disruption augments neutrophil transendothelial migration not through affecting the surface expression of adhesion molecules

We have shown that elevation of PIP₃ signaling via PTEN disruption led to enhanced neutrophil transendothelial migration. Because we used myeloid-specific PTEN KO mice, this enhancement was likely caused by PTEN depletion in neutrophils. One mechanism that is able to contribute to the increased transendothelial migration efficiency is the alteration of surface expression of cell adhesion molecules on neutrophils. To examine whether this variation was the case, we measured the surface expression level of several molecules involved in rolling, crawling, arrest, and emigration, including L-selectin, PSGL-1, CD44, CD11b, CD18, CD29, and CD31. Our results showed that nearly the same amount of these molecules was expressed in PTEN null and WT neutrophils (Fig. 8A). There was also no difference in the expression levels of CD11b, CD18, and CD29 on peritoneal neutrophils 4 h after thioglycolate peritoneal stimulation (data not shown). Because we recently demonstrated that PTEN deletion in neutrophils was associated with enhanced actin polymerization in response to fMLP stimulation *in vitro* (30), we paralleled by measuring

the cell surface expression of CD11b, an essential molecule for neutrophil crawling and adhesion, under similar stimulatory conditions. PTEN deletion had no influence on the cell surface expression of CD11b in response to fMLP over the in vitro stimulation period (Fig. 8B).

PTEN disruption augments chemokine-induced release of elastase and gelatinase from neutrophils

Neutrophil migration through endothelial cells and basement membrane is mediated by various junctional adhesion molecules, including PECAM-1, junctional adhesion molecules, $\alpha_6\beta_1$ integrin, ICAM-2, endothelial cell-selective adhesion molecule, CD99, VE-cadherin, and collagen (31, 40, 59, 60). It was previously reported that some neutrophil proteases, such as elastase and gelatinase, are capable of rapidly degrading components in the junctions and thus facilitate the neutrophil extravasation during an inflammatory response (61–66). These proteases are stored in granules in mature neutrophils. To perform their innate immune functions, neutrophils carry four major types of granules that evolve according to the neutrophil maturation stage and differ in their panel of markers. They are the primary, secondary, and tertiary granules and secretory vesicles. From the electron microscopy studies, we did not detect any difference in granule density or morphology between the WT and KO neutrophils (see supplemental Figs. S3 and S4).⁴ Neutrophils spreading over biological surfaces or transmigrating into inflamed tissue readily release granule components, including neutrophil elastase (elastase 2), and gelatinase B (MMP-9), upon activation. Thus, to further examine whether the altered protease release is responsible for the observed elevation of neutrophil transendothelial migration in the PTEN KO mice, we measured chemoattractant-elicited degranulation in WT and PTEN KO neutrophils. fMLP induced significant release of gelatinase from mouse neutrophils. Although the total amount of enzyme synthesized and stored in granules is the same between WT and PTEN null neutrophils, the amount of gelatinase released to the extracellular space increased by more than 3-fold in the neutrophils depleted of PTEN (Fig. 9A). A significant increase was also observed when the release of elastase was measured (Fig. 9B). These results suggested that disruption of PTEN significantly increased the release of elastase and gelatinase and this might be partially responsible for the enhanced neutrophil transendothelial migration in the PTEN KO mice.

Discussion

The tumor suppressor PTEN is a phosphatidylinositol 3'-phosphatase that converts PIP₃ to PIP₂. Depletion of this lipid phosphatase leads to accumulation of PIP₃ on the plasma membrane, and thus elevation of PIP₃ signaling. In this study, we report that myeloid-specific deletion of PTEN enhanced the neutrophil "invasivity" or emigration capability in inflammatory settings.

PIP₃ is a major downstream target of integrin and chemokine receptor, and has been implicated in multiple steps in leukocyte trafficking. Smith et al. (16) recently showed that disruption of PI3K γ , one of the PI3K-mediating G protein-coupled receptor signaling, interferes with integrin bond strengthening. PI3K γ null mice showed an 80% reduction in CXCL1 (KC)-induced leukocyte adhesion in venules of mouse cremaster muscle (16). Similar inhibition of tight adhesion was also observed when leukocyte transmigration from cremaster venules was induced with MIP-2 and TNF- α (17). Unexpectedly, we did not observe elevated leukocyte adhesion when the PIP₃ signaling was enhanced via PTEN depletion, suggesting that PIP₃ signaling is essential for stimuli-elicited cell adhesion, but not a limiting step for inducing elevated adhesion. Liu et al. (17) recently reported that leukocyte emigration was also substantially suppressed by inhibiting PI3K. Interestingly, it appears that the early response to MIP-2 or KC is mediated by PI3K γ , while the more

prolonged responses to MIP-2 or TNF- α is mediated by PI3K δ , a PI3K activated by receptor tyrosine kinase and integrin (17). In current study, disruption of PTEN elevated neutrophil emigration in both the early response to fMLP and prolonged responses to MIP-2 or TNF- α , suggesting that PTEN acts as a negative regulator in both processes. Most recently, Heit et al. (67) reported that under a certain situation, PTEN is required for prioritizing and integrating responses to multiple chemotactic cues. Disruption of PTEN leads to “distraction” in migrating neutrophils. Thus, the exact role of PTEN in neutrophils might rely on the diversity of chemoattractants involved, as well as the relative doses and route used to induce the neutrophil inflammatory reactions.

The elevated rolling velocities observed in the PTEN mice are somewhat surprising. Puri et al. (18, 19) recently reported that PIP₃ signaling can regulate neutrophil rolling by modulating the functions of endothelial cells, and both PI3K γ and PI3K δ played a critical role in E-selectin-mediated rolling in cremasteric venules in response to TNF- α . Nevertheless, the PTEN KO mice we used are myeloid-specific and contain WT endothelial cells. A previous report showed that PI3K deficiency in neutrophils had no effect on rolling flux or rolling velocity (17). The increased rolling velocity of PTEN null neutrophils might be indirectly caused by other alterations elicited by augmented PIP₃ signaling. Interestingly, we observed that microvilli on PTEN KO neutrophils are significantly longer than those on WT neutrophils (see supplemental Fig. S3),⁴ which is consistent with the elevated actin polymerization in the KO neutrophils (30). It is intriguing to examine whether the increased length of microvilli can lead to increased rolling velocity. We measured the surface expression of L-selectin and PSGL-1 on PTEN KO neutrophils and no significant changes were detected. However, we cannot rule out the possibility that augmentation of PIP₃ may alter the nature of PSGL-1 glycosylation, binding affinity, or its subsequent functions.

The neutrophil emigration can be divided into three stages: crawling, crossing vascular endothelial wall, and migration in the tissues, all of which are associated with actin polymerization-dependent cell polarization. After slow rolling, cells acquire the ability to polarize with clear head and tail formation. It is consistent for PTEN neutrophils, with enhanced actin polymerization and pseudopod formation in vitro, to show enhanced velocity in all the emigration stages in vivo, despite their WT expression level of β_1 and β_2 integrins, which are molecules needed for emigration. Neutrophils follow two paths to cross the vessel wall, the paracellular pathway through the interendothelial junctions and transcellular pathway across the endothelial cell itself (55, 56). Similar to what was previously reported (51, 68), we found that neutrophils predominantly use the paracellular pathway during their transendothelial migration. PTEN disruption did not alter the preference toward the paracellular pathway. Carman et al. suggested that the transcellular pathway is initiated by the presence of podosomes on the ventral part of the leukocytes to sense endothelial clues (69). Surprisingly, podosomes were equally present on both WT and KO neutrophils despite the predominant junctional pathway taken by these cells to emigrate (see supplemental Fig. S4).⁴ Despite the predominance of the paracellular pathway in neutrophil emigration, both WT and KO neutrophils displayed the podosome presence on their ventral side in touch with the endothelium. The podosome presence along with junctional dominance needs further investigation. It is noteworthy that in one experiment we used an Alexa Fluor 488-conjugated anti-PECAM-1 Ab to visualize the endothelial tight junctions. The injection of this Ab may modulate neutrophil recruitment. However, because only a relatively low concentration of Ab was used, its effect on neutrophil migration should be minimal. This response was confirmed by the normal neutrophil rolling, adhesion, and transmigration efficiency in mice injected with anti-PECAM-1 Ab. Importantly, the WT and KO mice were treated identically and studied in parallel in these experiments, so that any effects caused by Ab were well controlled for and the comparison of interest should in all cases be the effect of genetic deficiency.

Results from this study also suggest that the enhanced emigration of PTEN null neutrophils is likely due to alteration of intracellular signaling pathway because the surface expression of cell adhesion molecules involved in neutrophil trafficking was not changed on the PTEN KO neutrophils. The role of PTEN in regulating intracellular signaling in hemopoietic cells has been investigated in several other labs. Li et al. (70) demonstrated that PTEN intracellular localization and activity are regulated by chemoattractants through Rho GTPases, RhoA, and Cdc42. Immunostaining using a PTEN Ab showed PTEN localization at the back of stimulated neutrophils, along with RhoA. Transwell migration assays showed that knocking down PTEN levels in Jurkat T cells resulted in impaired chemotaxis. These results allowed the authors to propose the following function for PTEN in neutrophils, similar to the function proposed in *Dictyostelium* (71): localization of PTEN at the uropod locally inhibits PIP₃ production at the back of the cell and thereby confines PIP₃ production and actin polymerization to the leading edge of the cell and mediates directional sensing. Hence, disruption of PTEN would lead to uncontrolled propagation of PIP₃ at leading edge, causing formation of multiple pseudopodia, frequent direction changes and loss in directionality. Subsequently, another report suggested exactly the opposite function for PTEN. Gao et al. (26) proposed that PTEN actually suppresses chemotaxis and thus inhibition of PTEN enhances chemotactic migration. Interestingly, a third report came to a completely different conclusion from both of these studies. Lacalle et al. (28) used Jurkat T cells to show that PTEN does not affect chemotaxis, but only alters migration speed. Using myeloid-specific PTEN KO mice, we recently demonstrated that PTEN KO neutrophils were generally more sensitive to chemoattractants than were WT neutrophils and only had a subtle defect in directional migration (with an increase in migration speed). The PTEN KO neutrophils showed a more enhanced Transwell migration compared with WT neutrophils (30). Consistent with these in vitro results, in the current study, we observed a much-enhanced neutrophil emigration from cremasteric venules in the PTEN KO mice. Collectively, from our results we can conclude that PTEN does not play a role in directional sensing, but only regulates threshold for polarization and sensitivity in response to chemoattractants. It serves as a negative regulator for neutrophil transendothelial migration.

Although the enhanced transendothelial migration of PTEN null neutrophils can be simply explained by the increased sensitivity to chemoattractant and the elevated actin polymerization in response to extracellular stimuli, other mechanisms might also be responsible for the enhancement. It was previously reported that certain neutrophil proteases, including elastase and gelatinase, are capable of rapidly degrading junctional adhesion molecules such as PECAM-1, junctional adhesion molecules, $\alpha_6\beta_1$ integrin, ICAM, endothelial cell-selective adhesion molecule, CD99, VE-cadherin, and collagen and thus facilitate the neutrophil extravasation during an inflammatory response (61–66). Interestingly, we observed a significant elevation of chemoattractant-elicited release of neutrophil elastase and gelatinase from the PTEN null neutrophils (Fig. 9). Thus, the enhanced neutrophil extravasation in the KO mice could be partially contributed by the augmented protease-mediated degradation of components in the junctions. Enhanced transmigration can also be caused by alteration of neutrophil/endothelial or neutrophil/basement membrane interaction. However, electron microscopy examination revealed no obvious differences in the structures of neutrophil, vascular endothelial bed, basement membrane, as well as their interactions between the WT and PTEN KO mice (Fig. 5, and data not shown) (also see supplemental Figs. S3 and S4),⁴ indicating that the elevated transmigration in the PTEN KO mice is unlikely caused by the altered neutrophil/endothelial or neutrophil/basement membrane interaction. Lastly, several groups have recently reported that selectins can activate neutrophils and regulate neutrophil migration (72–75). However, our results showed that PIP₃/Akt pathway could not be modulated by E- or P-selectin, suggesting that PIP₃ is not a part of selectin-induced signaling (see supplemental Fig. S5).⁴ This result is consistent with previous reports that E-selectin elicited β_2 integrin activation in

neutrophils is mainly mediated by a MAPK pathway. Engagement of PSGL-1 by selectin enhances tyrosine phosphorylation and activates MAPK in neutrophils (72, 76, 77). In another report, it was shown that E-selectin binding to PSGL-1 can activate the β_2 integrin LFA-1 by signaling through spleen tyrosine kinase Syk. This signaling is independent of G protein-coupled receptors, and is mediated by an Src family kinase Fgr and an ITAM-containing adaptor proteins DAP12 (78). Collectively, published results and our own results suggest that the enhanced transendothelial migration of PTEN null neutrophils is unlikely due to the alteration of selectin-elicited signaling.

Supplementary Material

Refer to Web version on PubMed Central for supplementary material.

Acknowledgments

We thank Jian You for producing and maintaining mice and Louise Trakimas (Department of Cell Biology Harvard Medical School) for assistance in electron microscopy. We also thank Li Chai and John Manis for invaluable discussions.

References

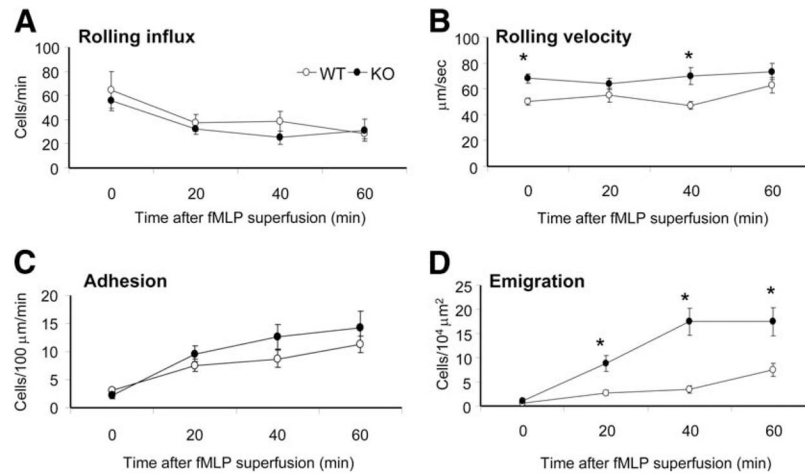
1. Bokoch GM. Chemoattractant signaling and leukocyte activation. *Blood*. 1995; 86:1649–1660. [PubMed: 7654998]
2. Devreotes PN, Zigmond SH. Chemotaxis in eukaryotic cells: a focus on leukocytes and Dictyostelium. *Annu Rev Cell Biol*. 1988; 4:649–686. [PubMed: 2848555]
3. Olson TS, Ley K. Chemokines and chemokine receptors in leukocyte trafficking. *Am J Physiol*. 2002; 283:R7–R28.
4. Katso R, Okkenhaug K, Ahmadi K, White S, Timms J, Waterfield MD. Cellular function of phosphoinositide 3-kinases: implications for development, homeostasis, and cancer. *Annu Rev Cell Dev Biol*. 2001; 17:615–675. [PubMed: 11687500]
5. Stephens L, Ellson C, Hawkins P. Roles of PI3Ks in leukocyte chemotaxis and phagocytosis. *Curr Opin Cell Biol*. 2002; 14:203–213. [PubMed: 11891120]
6. Ridley AJ, Schwartz MA, Burridge K, Firtel RA, Ginsberg MH, Borisy G, Parsons JT, Horwitz AR. Cell migration: integrating signals from front to back. *Science*. 2003; 302:1704–1709. [PubMed: 14657486]
7. Bourne HR, Weiner O. A chemical compass. *Nature*. 2002; 419:21. [PubMed: 12214215]
8. Shaw G. The pleckstrin homology domain: an intriguing multifunctional protein module. *Bioessays*. 1996; 18:35–46. [PubMed: 8593162]
9. Lemmon MA. Phosphoinositide recognition domains. *Traffic*. 2003; 4:201–213. [PubMed: 12694559]
10. Cantley LC. The phosphoinositide 3-kinase pathway. *Science*. 2002; 296:1655–1657. [PubMed: 12040186]
11. Rickert P, Weiner OD, Wang F, Bourne HR, Servant G. Leukocytes navigate by compass: roles of PI3K γ and its lipid products. *Trends Cell Biol*. 2000; 10:466–473. [PubMed: 11050418]
12. Corvera S, Czech MP. Direct targets of phosphoinositide 3-kinase products in membrane traffic and signal transduction. *Trends Cell Biol*. 1998; 8:442–446. [PubMed: 9854311]
13. Parent CA, Blacklock BJ, Froehlich WM, Murphy DB, Devreotes PN. G protein signaling events are activated at the leading edge of chemotactic cells. *Cell*. 1998; 95:81–91. [PubMed: 9778249]
14. Liliental J, Moon SY, Lesche R, Mamillapalli R, Li D, Zheng Y, Sun H, Wu H. Genetic deletion of the Pten tumor suppressor gene promotes cell motility by activation of Rac1 and Cdc42 GTPases. *Curr Biol*. 2000; 10:401–404. [PubMed: 10753747]
15. Camps M, Ruckle T, Ji H, Ardisson V, Rintelen F, Shaw J, Ferrandi C, Chabert C, Gillieron C, Francon B, et al. Blockade of PI3K γ suppresses joint inflammation and damage in mouse models of rheumatoid arthritis. *Nat Med*. 2005; 11:936–943. [PubMed: 16127437]

16. Smith DF, Deem TL, Bruce AC, Reutershan J, Wu D, Ley K. Leukocyte phosphoinositide-3 kinase γ is required for chemokine-induced, sustained adhesion under flow in vivo. *J Leukocyte Biol.* 2006; 80:1491–1499. [PubMed: 16997858]
17. Liu L, Puri KD, Penninger JM, Kubes P. Leukocyte PI3K γ and PI3K δ have temporally distinct roles for leukocyte recruitment in vivo. *Blood.* 2007; 110:1191–1198. [PubMed: 17488877]
18. Puri KD, Doggett TA, Douangpanya J, Hou Y, Tino WT, Wilson T, Graf T, Clayton E, Turner M, Hayflick JS, Diacovo TG. Mechanisms and implications of phosphoinositide 3-kinase δ in promoting neutrophil trafficking into inflamed tissue. *Blood.* 2004; 103:3448–3456. [PubMed: 14751923]
19. Puri KD, Doggett TA, Huang CY, Douangpanya J, Hayflick JS, Turner M, Penninger J, Diacovo TG. The role of endothelial PI3K γ activity in neutrophil trafficking. *Blood.* 2005; 106:150–157. [PubMed: 15769890]
20. Heit B, Liu L, Colarusso P, Puri KD, Kubes P. PI3K accelerates, but is not required for, neutrophil chemotaxis to fMLP. *J Cell Sci.* 2008; 121:205–214. [PubMed: 18187452]
21. Sasaki T, Irie-Sasaki J, Jones RG, Oliveira-dos-Santos AJ, Stanford WL, Bolon B, Wakeham A, Itie A, Bouchard D, et al. Function of PI3K γ in thymocyte development: T cell activation, and neutrophil migration. *Science.* 2000; 287:1040–1046. [PubMed: 10669416]
22. Hirsch E V, Katanaev L, Garlanda C, Azzolino O, Pirola L, Silengo L, Sozzani S, Mantovani A, Altruda F, Wymann MP. Central role for G protein-coupled phosphoinositide 3-kinase γ in inflammation. *Science.* 2000; 287:1049–1053. [PubMed: 10669418]
23. Li J, Yen C, Liaw D, Podsypanina K, Bose S, Wang SI, Puc J, Miliareis C, Rodgers L, McCombie R, et al. PTEN, a putative protein tyrosine phosphatase gene mutated in human brain, breast, and prostate cancer. *Science.* 1997; 275:1943–1947. [PubMed: 9072974]
24. Steck PA, Pershouse MA, Jasser SA, Yung WK, Lin H, Ligon AH, Langford LA, Baumgard ML, Hattier T, Davis T, et al. Identification of a candidate tumour suppressor gene: MMAC1, at chromosome 10q23.3 that is mutated in multiple advanced cancers. *Nat Genet.* 1997; 15:356–362. [PubMed: 9090379]
25. Maehama T, Dixon JE. PTEN: a tumour suppressor that functions as a phospholipid phosphatase. *Trends Cell Biol.* 1999; 9:125–128. [PubMed: 10203785]
26. Gao P, Wange RL, Zhang N, Oppenheim JJ, Howard OM. Negative regulation of CXCR4-mediated chemotaxis by the lipid phosphatase activity of tumor suppressor PTEN. *Blood.* 2005; 106:2619–2626. [PubMed: 15994292]
27. Kwak YG, Song CH, Yi HK, Hwang PH, Kim JS, Lee KS, Lee YC. Involvement of PTEN in airway hyperresponsiveness and inflammation in bronchial asthma. *J Clin Invest.* 2003; 111:1083–1092. [PubMed: 12671058]
28. Lacalle RA, Gomez-Mouton C, Barber DF, Jimenez-Baranda S, Mira E, Martinez AC, Carrera AC, Manes S. PTEN regulates motility but not directionality during leukocyte chemotaxis. *J Cell Sci.* 2004; 117:6207–6215. [PubMed: 15564381]
29. Tamura M, Gu J, Matsumoto K, Aota S, Parsons R, Yamada KM. Inhibition of cell migration, spreading, and focal adhesions by tumor suppressor PTEN. *Science.* 1998; 280:1614–1617. [PubMed: 9616126]
30. Subramanian KK, Jia Y, Zhu D, Simms BT, Jo H, Hattori H, You J, Mizgerd JP, Luo HR. Tumor suppressor PTEN is a physiologic suppressor of chemoattractant-mediated neutrophil functions. *Blood.* 2007; 109:4028–4037. [PubMed: 17202315]
31. Muller WA. Leukocyte-endothelial-cell interactions in leukocyte transmigration and the inflammatory response. *Trends Immunol.* 2003; 24:327–334. [PubMed: 12810109]
32. Springer TA. Traffic signals for lymphocyte recirculation and leukocyte emigration: the multistep paradigm. *Cell.* 1994; 76:301–314. [PubMed: 7507411]
33. Foxman EF, Campbell JJ, Butcher EC. Multistep navigation and the combinatorial control of leukocyte chemotaxis. *J Cell Biol.* 1997; 139:1349–1360. [PubMed: 9382879]
34. Wagner JG, Roth RA. Neutrophil migration mechanisms, with an emphasis on the pulmonary vasculature. *Pharmacol Rev.* 2000; 52:349–374. [PubMed: 10977867]
35. Simon SI, Green CE. Molecular mechanics and dynamics of leukocyte recruitment during inflammation. *Annu Rev Biomed Eng.* 2005; 7:151–185. [PubMed: 16004569]

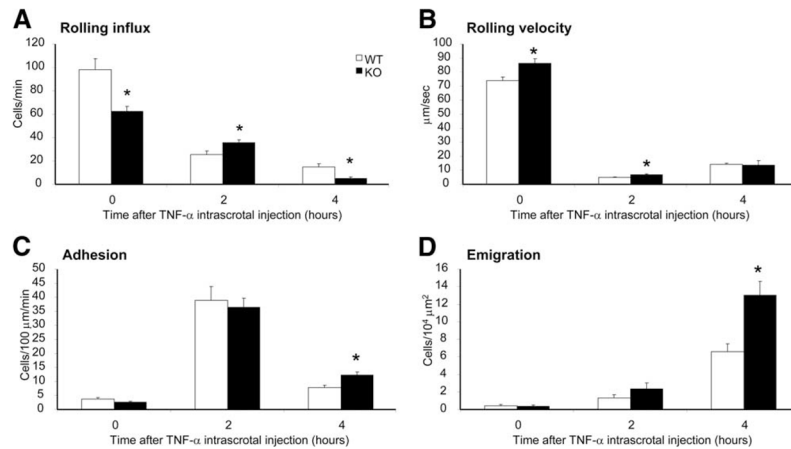
36. von Andrian UH, Arfors KE. Neutrophil-endothelial cell interactions in vivo: a chain of events characterized by distinct molecular mechanisms. *Agents Actions Suppl.* 1993; 41:153–164. [PubMed: 8317339]
37. Luster AD, Alon R, von Andrian UH. Immune cell migration in inflammation: present and future therapeutic targets. *Nat Immunol.* 2005; 6:1182–1190. [PubMed: 16369557]
38. von Andrian UH, Chambers JD, McEvoy LM, Bargatze RF, Arfors KE, Butcher EC. Two-step model of leukocyte-endothelial cell interaction in inflammation: distinct roles for LECAM-1 and the leukocyte $\beta 2$ integrins in vivo. *Proc Natl Acad Sci USA.* 1991; 88:7538–7542. [PubMed: 1715568]
39. Springer TA. Traffic signals on endothelium for lymphocyte recirculation and leukocyte emigration. *Annu Rev Physiol.* 1995; 57:827–872. [PubMed: 7778885]
40. Ley K, Laudanna C, Cybulsky MI, Nourshargh S. Getting to the site of inflammation: the leukocyte adhesion cascade updated. *Nat Rev Immunol.* 2007; 7:678–689. [PubMed: 17717539]
41. Zhu D, Hattori H, Jo H, Jia Y, Subramanian KK, Loison F, You J, Le Y, Honczarenko M, Silberstein L, Luo HR. Deactivation of phosphatidylinositol 3,4,5-trisphosphate/Akt signaling mediates neutrophil spontaneous death. *Proc Natl Acad Sci USA.* 2006; 103:14836–14841. [PubMed: 16988010]
42. Weninger W, Carlsen HS, Goodarzi M, Moazed F, Crowley MA, Bækkevold ES, Cavanagh LL, von Andrian UH. Naive T cell recruitment to nonlymphoid tissues: a role for endothelium-expressed CC chemokine ligand 21 in autoimmune disease and lymphoid neogenesis. *J Immunol.* 2003; 170:4638–4648. [PubMed: 12707342]
43. Coxon A, Rieu P, Barkalow FJ, Askari S, Sharpe AH, von Andrian UH, Arnaout MA, Mayadas TN. A novel role for the $\beta 2$ integrin CD11b/CD18 in neutrophil apoptosis: a homeostatic mechanism in inflammation. *Immunity.* 1996; 5:653–666. [PubMed: 8986723]
44. Ley K, Bullard DC, Arbones ML, Bosse R, Vestweber D, Tedder TF, Beaudet AL. Sequential contribution of L- and P-selectin to leukocyte rolling in vivo. *J Exp Med.* 1995; 181:669–675. [PubMed: 7530761]
45. Khadaroo RG, He R, Parodo J, Powers KA, Marshall JC, Kapus A, Rotstein OD. The role of the Src family of tyrosine kinases after oxidant-induced lung injury in vivo. *Surgery.* 2004; 136:483–488. [PubMed: 15300219]
46. Kanwar S, Hickey MJ, Kubes P. Postischemic inflammation: a role for mast cells in intestine but not in skeletal muscle. *Am J Physiol.* 1998; 275:G212–G218. [PubMed: 9688647]
47. Woodfin A, Reichel CA, Khandoga A, Corada M, Voisin MB, Scheiermann C, Haskard DO, Dejana E, Krombach F, Nourshargh S. JAM-A mediates neutrophil transmigration in a stimulus-specific manner in vivo: evidence for sequential roles for JAM-A and PECAM-1 in neutrophil transmigration. *Blood.* 2007; 110:1848–1856. [PubMed: 17505016]
48. Smith ML, Smith MJ, Lawrence MB, Ley K. Viscosity-independent velocity of neutrophils rolling on P-selectin in vitro or in vivo. *Microcirculation.* 2002; 9:523–536. [PubMed: 12483549]
49. Forlow SB, Ley K. Selectin-independent leukocyte rolling and adhesion in mice deficient in E-, P-, and L-selectin and ICAM-1. *Am J Physiol.* 2001; 280:H634–H641.
50. Liu L, Cara DC, Kaur J, Raharjo E, Mullaly SC, Jongstra-Bilen J, Jongstra J, Kubes P. LSP1 is an endothelial gatekeeper of leukocyte transendothelial migration. *J Exp Med.* 2005; 201:409–418. [PubMed: 15684321]
51. Phillipson M, Heit B, Colarusso P, Liu L, Ballantyne CM, Kubes P. Intraluminal crawling of neutrophils to emigration sites: a molecularly distinct process from adhesion in the recruitment cascade. *J Exp Med.* 2006; 203:2569–2575. [PubMed: 17116736]
52. Zhang XW, Wang Y, Liu Q, Thorlacius H. Redundant function of macrophage inflammatory protein-2 and KC in tumor necrosis factor- α -induced extravasation of neutrophils in vivo. *Eur J Pharmacol.* 2001; 427:277–283. [PubMed: 11567658]
53. Auffray C, Fogg D, Garfa M, Elain G, Join-Lambert O, Kayal S, Sarnacki S, Cumano A, Lauvau G, Geissmann F. Monitoring of blood vessels and tissues by a population of monocytes with patrolling behavior. *Science.* 2007; 317:666–670. [PubMed: 17673663]
54. Schenkel AR, Mamdouh Z, Muller WA. Locomotion of monocytes on endothelium is a critical step during extravasation. *Nat Immunol.* 2004; 5:393–400. [PubMed: 15021878]

55. Vestweber D. Adhesion and signaling molecules controlling the transmigration of leukocytes through endothelium. *Immunol Rev.* 2007; 218:178–196. [PubMed: 17624953]
56. Nourshargh S, Marelli-Berg FM. Transmigration through venular walls: a key regulator of leukocyte phenotype and function. *Trends Immunol.* 2005; 26:157–165. [PubMed: 15745858]
57. Feng D, Nagy JA, Pyne K, Dvorak HF, Dvorak AM. Ultra-structural localization of platelet endothelial cell adhesion molecule (PECAM-1, CD31) in vascular endothelium. *J Histochem Cytochem.* 2004; 52:87–101. [PubMed: 14688220]
58. Seal JB, Gewertz BL. Vascular dysfunction in ischemia-reperfusion injury. *Ann Vasc Surg.* 2005; 19:572–584. [PubMed: 15981128]
59. Petri B, Phillipson M, Kubes P. The physiology of leukocyte recruitment: an in vivo perspective. *J Immunol.* 2008; 180:6439–6446. [PubMed: 18453558]
60. Weber C, Fraemohs L, Dejana E. The role of junctional adhesion molecules in vascular inflammation. *Nat Rev Immunol.* 2007; 7:467–477. [PubMed: 17525755]
61. Wang S, Dangerfield JP, Young RE, Nourshargh S. PECAM-1, alpha6 integrins and neutrophil elastase cooperate in mediating neutrophil transmigration. *J Cell Sci.* 2005; 118:2067–2076. [PubMed: 15840647]
62. Allport JR, Ding H, Collins T, Gerritsen ME, Luscinskas FW. Endothelial-dependent mechanisms regulate leukocyte transmigration: a process involving the proteasome and disruption of the vascular endothelial-cadherin complex at endothelial cell-to-cell junctions. *J Exp Med.* 1997; 186:517–527. [PubMed: 9254650]
63. Moll T, Dejana E, Vestweber D. In vitro degradation of endothelial catenins by a neutrophil protease. *J Cell Biol.* 1998; 140:403–407. [PubMed: 9442115]
64. Reichel CA, Rehberg M, Bihari P, Moser CM, Linder S, Khandoga A, Krombach F. Gelatinases mediate neutrophil recruitment in vivo: evidence for stimulus specificity and a critical role in collagen IV remodeling. *J Leukocyte Biol.* 2008; 83:864–874. [PubMed: 18174361]
65. Ducharme A, Frantz S, Aikawa M, Rabkin E, Lindsey M, Rohde LE, Schoen FJ, Kelly RA, Werb Z, Libby P, Lee RT. Targeted deletion of matrix metalloproteinase-9 attenuates left ventricular enlargement and collagen accumulation after experimental myocardial infarction. *J Clin Invest.* 2000; 106:55–62. [PubMed: 10880048]
66. Renckens R, Roelofs JJ, Florquin S, de Vos AF, Lijnen HR, van't Veer C, van der Poll T. Matrix metalloproteinase-9 deficiency impairs host defense against abdominal sepsis. *J Immunol.* 2006; 176:3735–3741. [PubMed: 16517742]
67. Heit B, Robbins SM, Downey CM, Guan Z, Colarusso P, Miller BJ, Jirik FR, Kubes P. PTEN functions to 'prioritize' chemotactic cues and prevent 'distraction' in migrating neutrophils. *Nat Immunol.* 2008; 9:743–752. [PubMed: 18536720]
68. Wojciechowski JC I, Sarelius H. Preferential binding of leukocytes to the endothelial junction region in venules in situ. *Microcirculation.* 2005; 12:349–359. [PubMed: 16020081]
69. Carman CV, Sage PT, Sciuto TE, de la Fuente MA, Geha RS, Ochs HD, Dvorak HF, Dvorak AM, Springer TA. Transcellular diapedesis is initiated by invasive podosomes. *Immunity.* 2007; 26:784–797. [PubMed: 17570692]
70. Li Z, Dong X, Wang Z, Liu W, Deng N, Ding Y, Tang L, Hla T, Zeng R, Li L, Wu D. Regulation of PTEN by Rho small GTPases. *Nat Cell Biol.* 2005; 7:399–404. [PubMed: 15793569]
71. Iijima M, Devreotes P. Tumor suppressor PTEN mediates sensing of chemoattractant gradients. *Cell.* 2002; 109:599–610. [PubMed: 12062103]
72. Simon SI, Hu Y, Vestweber D, Smith CW. Neutrophil tethering on E-selectin activates $\beta 2$ integrin binding to ICAM-1 through a mitogen-activated protein kinase signal transduction pathway. *J Immunol.* 2000; 164:4348–4358. [PubMed: 10754335]
73. Hidalgo A, Peired AJ, Wild MK, Vestweber D, Frenette PS. Complete identification of E-selectin ligands on neutrophils reveals distinct functions of PSGL-1, ESL-1, and CD44. *Immunity.* 2007; 26:477–489. [PubMed: 17442598]
74. Zarbock A, Lowell CA, Ley K. Spleen tyrosine kinase Syk is necessary for E-selectin-induced $\alpha L \beta 2$ integrin-mediated rolling on intercellular adhesion molecule-1. *Immunity.* 2007; 26:773–783. [PubMed: 17543554]

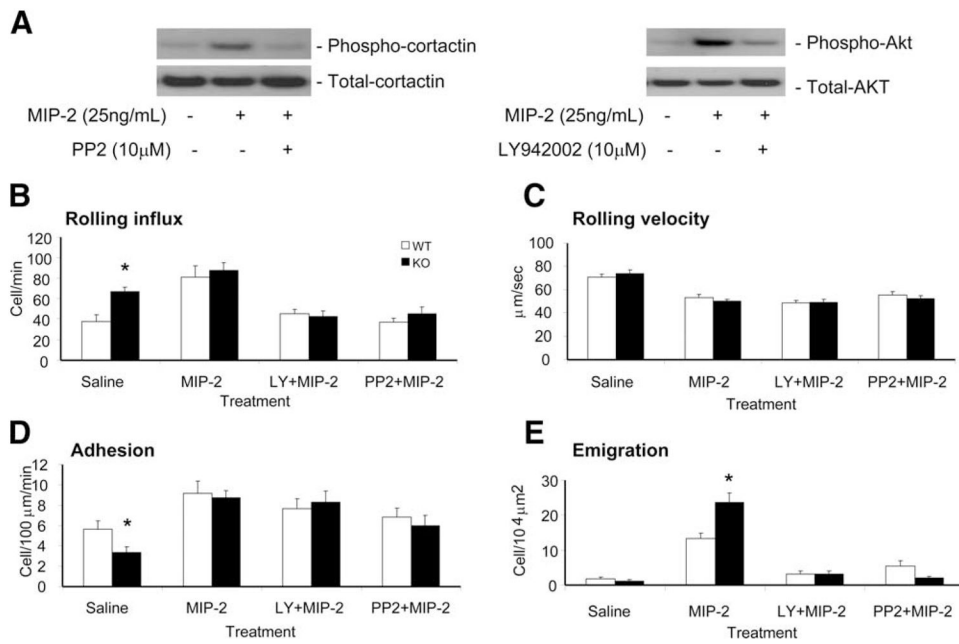
75. Miner JJ, Xia L, Yago T, Kappelmayer J, Liu Z, Klopocki AG, Shao B, McDaniel JM, Setiadi H, Schmidtke DW, McEver RP. Separable requirements for cytoplasmic domain of PSGL-1 in leukocyte rolling and signaling under flow. *Blood*. 2008; 112:2035–2045. [PubMed: 18550846]
76. Hidari KI, Weyrich AS, Zimmerman GA, McEver RP. Engagement of P-selectin glycoprotein ligand-1 enhances tyrosine phosphorylation and activates mitogen-activated protein kinases in human neutrophils. *J Biol Chem*. 1997; 272:28750–28756. [PubMed: 9353345]
77. Waddell TK, Fialkow L, Chan CK, Kishimoto TK, Downey GP. Signaling functions of L-selectin: enhancement of tyrosine phosphorylation and activation of MAP kinase. *J Biol Chem*. 1995; 270:15403–15411. [PubMed: 7541041]
78. Zarbock A, Abram CL, Hundt M, Altman A, Lowell CA, Ley K. PSGL-1 engagement by E-selectin signals through Src kinase Fgr and ITAM adapters DAP12 and FcR γ to induce slow leukocyte rolling. *J Exp Med*. 2008; 205:2339–2347. [PubMed: 18794338]

**FIGURE 1.**

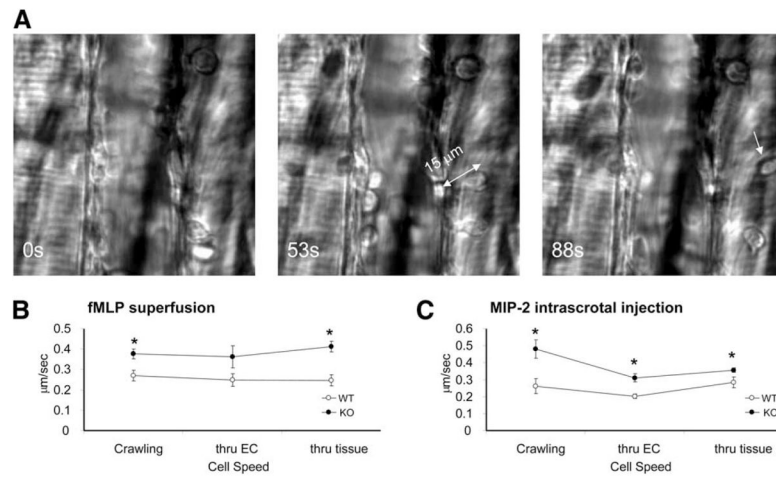
PTEN KO neutrophils display enhanced emigration in response to fMLP superfusion. Leukocyte recruitment was induced by a continuous flow of 35°C thermally stable saline (0 min) then 10 μ M fMLP (20, 40, and 60 min). The major trafficking parameters, which are the rolling flux (A), rolling velocity (B), adhesion or sticking (C), and emigration (D) were determined in the postcapillary venules of the mouse cre-master for $n = 3$ mice per genotype. *, $p < 0.05$ between WT and corresponding PTEN KO mice.

**FIGURE 2.**

TNF- α stimulation leads to enhanced emigration of PTEN KO neutrophils. Leukocyte recruitment was induced by an intrascrotal injection of 0.5 μ g of TNF- α in 300 μ l of saline solution. Recordings were taken at time points 0 (no injection), 2, and 4 h (TNF- α postinjection) under continuous flow of 35°C thermally stable saline. The major trafficking parameters, which are the rolling flux (A), rolling velocity (B), adhesion or sticking (C), and emigration (D) were determined in the postcapillary cremasteric venules for $n = 3$ mice per genotype. *, $p < 0.05$ between WT and PTEN KO mice.

**FIGURE 3.**

Induction of neutrophil recruitment by MIP-2 intrascrotal injection in the presence or absence of PI3K and Src kinase inhibition. *A*, PI3K and Src kinase activities can be inhibited by specific inhibitors. Neutrophils isolated from WT mice were incubated with 25 ng/ml MIP-2 in the presence of indicated inhibitors for 10 min. Phosphorylated and total Akt were detected by Western blotting using anti-phospho-Akt Ab (Ser⁴⁷³) (1/1000) and anti-Akt Abs (1/1000) (Cell Signaling Technology), respectively. Similarly, Src activity was determined by measuring phosphorylation of cortactin, a well-known downstream factor in the Src signaling pathway. *B–E*, Leukocyte recruitment was stimulated by an intrascrotal injection of 300 μ l of saline or 1 μ g of MIP-2 in 300 μ l of saline solution. In separate experiments, the MIP-2 intrascrotal injection was 20 min preceded by an i.p. injection of 10 mg/kg PI3K inhibitor LY942002 or 0.2 mg/kg Src inhibitor PP2. Recordings were taken 2 h after the intrascrotal injection under continuous flow of 35°C thermally stable saline. The major trafficking parameters, which are the rolling flux (*B*), rolling velocity (*C*), adhesion or sticking (*D*), and emigration (*E*) were determined in the postcapillary venules of the mouse cremaster for $n = 3$ mice per genotype. *, $p < 0.05$ between WT and PTEN KO animals.

**FIGURE 4.**

PTEN KO neutrophils display faster crawling and emigration across the postcapillary venular wall and through muscle tissue. *A*, Still images showing a cell crossing the vascular endothelial wall, before the cell starts emigration (*left*), after the complete cell detachment off the abluminal side of the vessel (*middle*), and after the cell is far from the vessel (*right*). Indicated time is in seconds. Magnification is $\times 100$. The two-head arrow (*middle*) indicates the length of the cell. The arrow in the *right* image points to the same cell in the *middle* image, now away from the vessel. Leukocyte recruitment was stimulated by superfusion with $10 \mu\text{M}$ fMLP (*B*) or intrascrotal injection of $1 \mu\text{g}$ of MIP-2 in $300 \mu\text{l}$ of saline solution (*C*). Crawling cells were identified by their polarized shape as well as their lateral migration across the vessel bed. At least $n = 3$ mice per genotype were analyzed. *, $p < 0.05$.

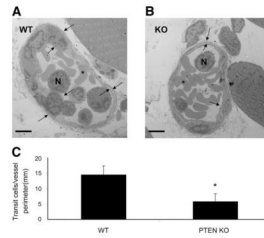
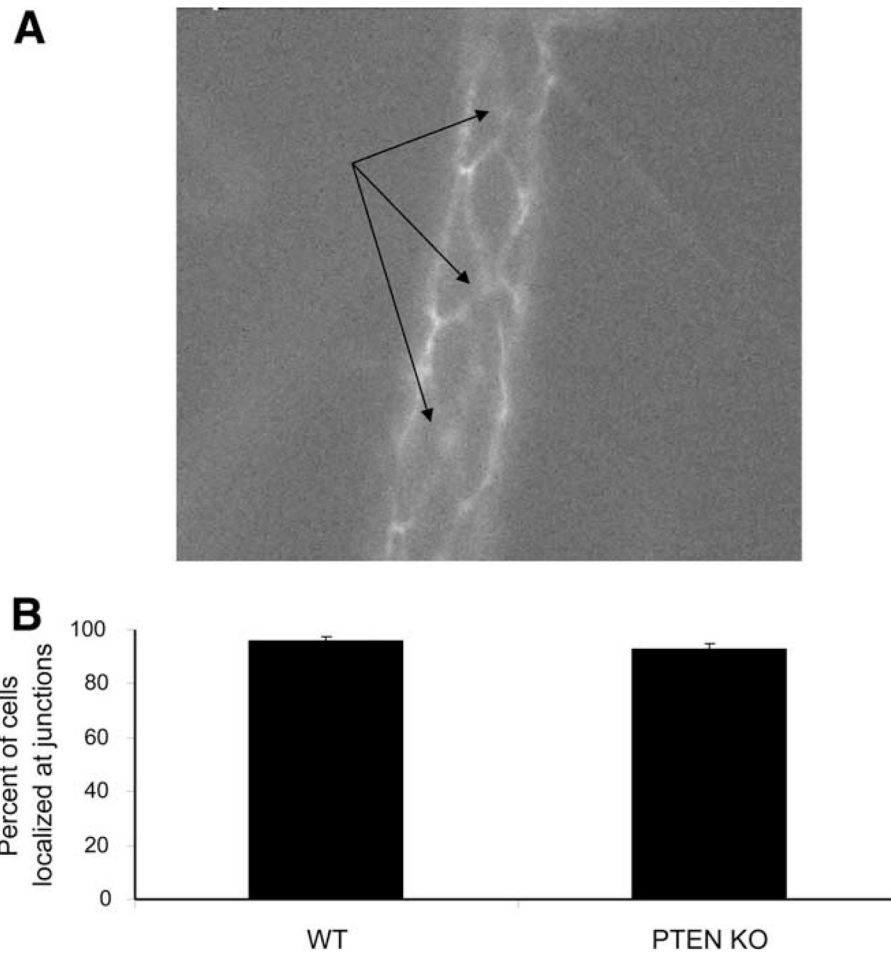
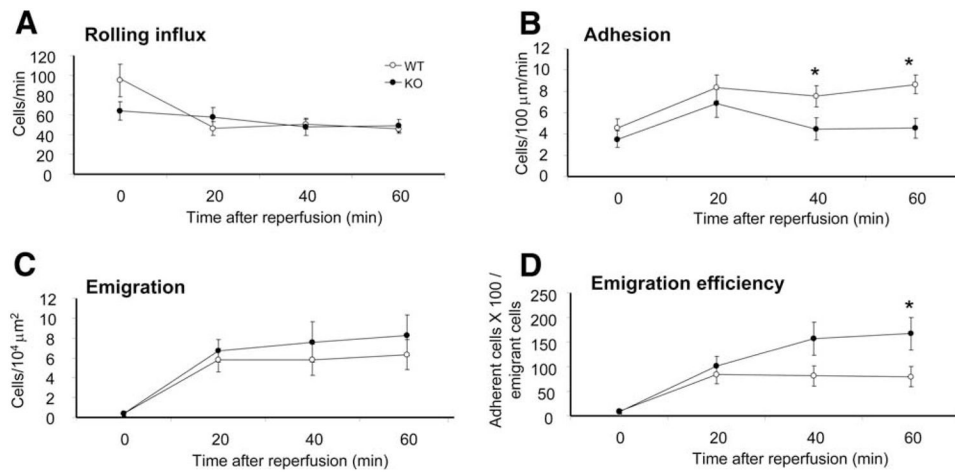


FIGURE 5.

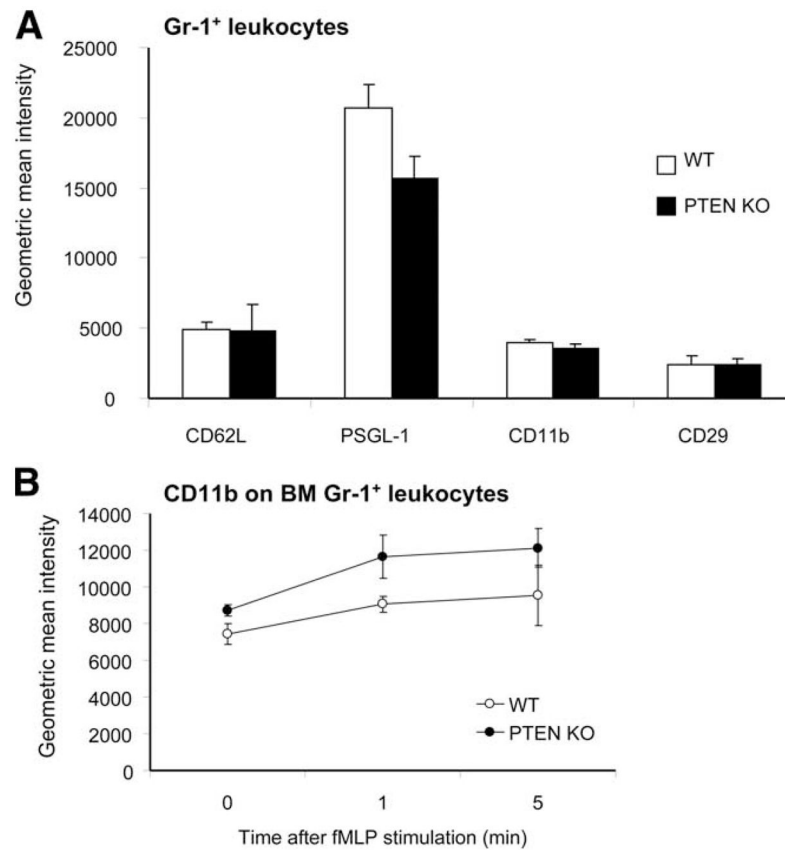
WT neutrophils are being held up between vascular endothelium and basement membrane. WT or PTEN KO mice were intrascrotally injected with 1 μ g MIP-2. Three hours later, the cremaster muscle was fixed in a fixing buffer (see *Materials and Methods*) and prepared for electron microscopy. A cross-section of WT (A) and KO (B) postcapillary venule shows neutrophils (N), RBC (asterisk), the vascular endothelial layer (inside arrows), and the basement membrane/pericyte layer (outside arrow). Scale bar represents 5 μ m. C, The number of abluminal leukocytes per vessel perimeter; these cells crossed the endothelium but stayed on its abluminal side. *, $p < 0.05$. At least 18 vessel sections were analyzed. Magnification is $\times 1400$ (A) and $\times 1200$ (B).

**FIGURE 6.**

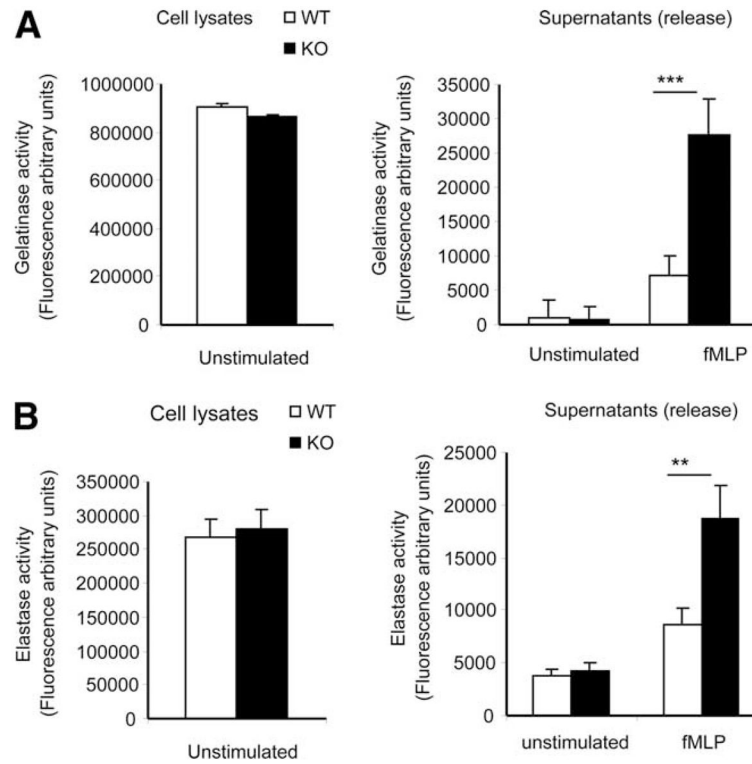
Enhanced emigration of PTEN neutrophils does not necessarily enhance the transcellular pathway. Leukocyte recruitment was stimulated by a continuous flow of 35°C thermally stable 10 μ M fMLP in saline. Twenty minutes later, 40 μ g of Alexa Fluor 488-conjugated anti-CD31 (PECAM-1) mAb was i.v. introduced. *A*, A video caption of a WT postcapillary venule. *B*, Percentage of adherent cells that localized to endothelial boundaries in both WT and PTEN KO cremaster vessel beds. Arrow points to silhouettes of leukocytes localized to interendothelial junctions for $n = 2$ WT and $n = 3$ KO mice.

**FIGURE 7.**

PTEN KO neutrophils are more efficient in postreperfusion emigration. Leukocyte recruitment was stimulated with 30-min ischemia; blood flow blockage was detected under IVM. Reperfusion follows as blood flow continued for 60 min and trafficking parameters were observed at 20-, 40-, and 60-min time points. Time point 0 represents the condition before applying ischemia to the muscle. Continuous superfusion of thermostable saline was applied for both ischemia and reperfusion. *A*, The number of rolling cells that passed an imaginary cross-section of the vessel per minute. *B*, The number of adherent cells that stayed stationary for at least 30 s within a 100- μm long vessel. *C*, The number of emigrating cells within a distance of 50 μm from the 100- μm long vessels on both sides. *D*, Emigration efficiency is defined as the percentage of adherent cells able to emigrate for $n = 4$ mice per genotype. *, $p < 0.05$.

**FIGURE 8.**

Adhesion molecule expression on GR-1-positive leukocytes. *A*, Peripheral blood leukocytes were double-labeled with FITC-conjugated anti-Gr-1 and PE-conjugated anti-adhesion molecule or one of the indicated adhesion molecules. *B*, Bone marrow leukocytes were stimulated with 100 nM fMLP, then labeled with PE-conjugated anti-CD11b and FITC-conjugated anti-Gr-1 for $n = 3$ mice per genotype.

**FIGURE 9.**

PTEN disruption increases chemoattractant-induced release of elastase and gelatinase from neutrophils. Neutrophils isolated from PTEN KO and WT mice were stimulated with $1 \mu\text{M}$ fMLP for 30 min at 37°C . Supernatants were harvested, and gelatinase (A) and elastase (B) activities in the supernatants were measured using an EnzChek Gelatinase Assay kit and an EnzCheck Elastase Assay kit, respectively. Cell lysates of the same number of unstimulated neutrophils were used to measure the total amount of intracellular gelatinase and elastase activity. Data are presented as mean \pm SD ($n = 3$ mice). *, $p < 0.05$ vs WT mice. **, $p < 0.01$ vs WT mice. ***, $p < 0.005$ vs WT mice.